

See discussions, stats, and author profiles for this publication at: <https://www.researchgate.net/publication/267273242>

DFT and ENDOR Study of Bixin Radical Cations and Neutral Radicals on Silica-Alumina

ARTICLE *in* THE JOURNAL OF PHYSICAL CHEMISTRY B · OCTOBER 2014

Impact Factor: 3.3 · DOI: 10.1021/jp506806n · Source: PubMed

READS

26

5 AUTHORS, INCLUDING:



Michael K. Bowman

University of Alabama

179 PUBLICATIONS 3,836 CITATIONS

[SEE PROFILE](#)



Lowell D Kispert

University of Alabama

278 PUBLICATIONS 3,923 CITATIONS

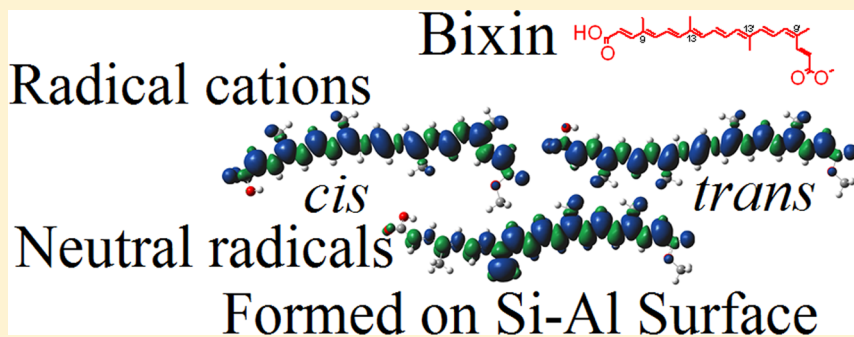
[SEE PROFILE](#)

DFT and ENDOR Study of Bixin Radical Cations and Neutral Radicals on Silica–Alumina

Sefadzi S. Tay-Agbozo, Matthew D. Krzyaniak,[†] Michael K. Bowman, Shane Street, and Lowell D. Kispert*

Department of Chemistry, The University of Alabama, Box 870336, Tuscaloosa, Alabama 35487-0336, United States

Supporting Information



ABSTRACT: Bixin, a carotenoid found in annatto (*Bixa orellana*), is unique among natural carotenoids by being water-soluble. We stabilized free radicals from bixin on the surface of silica–alumina (Si–Al) and characterized them by pulsed electron–nuclear double resonance (ENDOR). DFT calculations of unpaired electron spin distribution for various bixin radicals predict the EPR hyperfine couplings. Least-square fitting of experimental ENDOR spectra by spectra calculated from DFT hyperfine couplings characterized the radicals trapped on Si–Al. DFT predicts that the *trans* bixin radical cation is more stable than the *cis* bixin radical cation by 1.26 kcal/mol. This small energy difference is consistent with the 26% *trans* and 23% *cis* radical cations in the ENDOR spectrum. The remainder of the ENDOR spectrum is due to several neutral radicals formed by loss of a H⁺ ion from the 9, 9', 13, or 13' methyl group, a common occurrence in all water-insoluble carotenoids previously studied. Although carboxyl groups of bixin strongly affect its solubility relative to other natural carotenoids, they do not alter properties of its free radicals based on DFT calculations and EPR measurements which remain similar to typical water-insoluble carotenoids.

INTRODUCTION

Carotenoids are pigments responsible for the color of many fruits and vegetables. Nearly all carotenoids can be derived from lycopene, Figure 1a, the red pigment in ripe tomato fruit. The numbering system of bixin and other carotenoids, e.g., 9(9') and 13(13') methyl groups, is defined relative to the structure

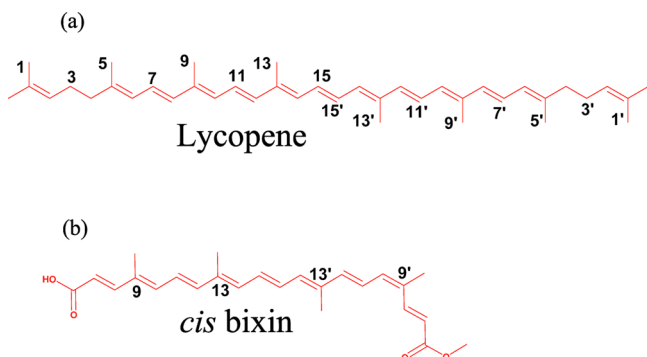


Figure 1. (a) Lycopene, the compound from which most carotenoids can be derived, and (b) *cis* bixin; note that it is not symmetric, with –COOH at one end and –COOCH₃ at the other.

of lycopene. Bixin, (2E,4E,6E,8E,10E,12E,14E,16Z,18E)-20-methoxy-4,8,13,17-tetramethyl-20-oxoicosa-2,4,6,8,10,12,14,16,18-nonaenoic acid, is the main carotenoid found in the seed of annatto—*Bixa orellana*, named after the conquistador Francisco de Orellana¹—and accounts for over 80% of all the carotenoids found in annatto. Annatto is derived from the seeds of the tropical achiote trees.^{1–9} The backbone of carotenoids consists of a conjugated π-system with the π-electrons delocalized along the chain. These conjugated double bonds impart several characteristic qualities to carotenoids. Carotenoids are not photochemically reactive, because the optical transition concerns S₀–S₂, followed by fast internal conversion to S₁ with a lifetime of 10–50 ps, thus drastically reducing the available energy for photochemistry. Carotenoids can undergo fast photochemical reactions such as photoinduced electron transfer into the conduction band of a semiconductor as for the carotenoic acid solar cell.¹⁰ Like most carotenoids, bixin is an efficient quencher of singlet-state oxygen and of the

Special Issue: John R. Miller and Marshall D. Newton Festschrift

Received: July 8, 2014

Revised: October 1, 2014

triplet state of sensitizers¹¹ and has a great capacity to scavenge reactive oxygen and nitrogen species.¹² Generally, carotenoids are hydrophobic and soluble in organic solvents but have very limited solubility in water. Bixin is the exception, combining large extinction coefficient, water solubility, and limited photochemistry.

Bixin was first isolated in 1825 with the first crystallization reported in 1878.¹ It is only present in the coat of the annatto seed, not the entire seed. Although bixin or annatto has been used extensively in the food, beverage,^{3,4,6,9,13–16} and pharmaceutical/cosmetic^{2,6,11,15,17} industries, not much is known of its electron transfer properties or subsequent reactions of its radical cation. The extensive use of annatto in foods, beverages, pharmaceuticals, and cosmetics is thought to be more for appearance than for its nutrition or medicinal properties.⁷ Commercial production of annatto makes bixin an attractive source for large amounts of water-soluble carotenoid.

Carotenoid radical cations can be formed by electron transfer from the carotenoid to Lewis acid sites on a surface. The radical cation is a weak acid¹⁸ ($pK_a = 4–7$) that can lose a H^+ to form neutral radicals. These radicals are part of the photoprotection mechanism in plant photosynthesis¹⁹ and combat oxidative damage and aging.^{20,21} It is possible to stabilize carotenoid radicals on activated Si–Al, allowing long-term studies of the free radicals to characterize their unpaired spin density distribution and conformation. The Si–Al is calcined to partially dehydrate the surface and form a variety of Lewis acid and Bronsted acid sites on the surface which are partially the basis for the industrial use of Si–Al as a catalyst.²² The structure and properties of active surface sites of metal oxides are an active area of catalysis research²³ and well beyond the scope of this article. However, activated Si–Al is a convenient tool for generating and stabilizing carotenoid radicals for subsequent spectroscopic studies to identify and characterize the radicals.^{24–28} However, the radicals must remain isolated from reactive molecules such as O_2 , H_2O , and other carotenoid molecules, which is done here by flame sealing the EPR tubes under a vacuum and storing them at 77 K to prevent diffusion of radicals and other carotenoids along the surface of the Si–Al.

Even though the interaction with the Si–Al surface helps stabilize carotenoid radicals, it does not seem to cause significant distortions in the ground state electronic structure. To date, there have been no significant changes in hyperfine couplings or unpaired spin density distribution in any of the carotenoids studied whether they were stabilized on Si–Al, supported on the MCM-41 surface, or frozen in solution.²⁹ In this respect, the carotenoid radicals are extremely poor reporters for probing active sites on metal oxide surfaces because they do not show any significant hyperfine couplings to the oxide surface. In contrast, with some radical probes, we do see large hyperfine couplings to the oxide surface.^{30,31}

Photovoltaic cells have been constructed from synthetic carotenoic acid on TiO_2 nanocrystalline mesoporous electrodes.¹⁰ Bixin contains a carboxylic group on one end and an ester on the other (Figure 1b) and could be a natural source of materials for a photovoltaic cell. The carotenoid in a photovoltaic cell functions as an electron donor, transiently forming a radical cation that may undergo further reaction such as loss of H^+ to form neutral radicals. On the basis of experience with other carotenoid radical cations, H^+ loss is most likely to occur from one of the four methyl groups along the hydrocarbon backbone of bixin, with the most stable radicals being found in the highest amount.^{24,26} However, the

free radicals of carotenoids with a polar, potentially charged group, such as the carboxyl group of bixin, have never been examined. Polar groups that confer water solubility also have the potential to affect the relative stability of radicals formed by H^+ loss from the hydrocarbon chain and alter the normal pattern of radical products seen in other carotenoids. This study examines the bixin radical cations and subsequent neutral radicals stabilized on Si–Al to understand the free radical reactions of this novel, natural carotenoid with an unusual combination of properties: large extinction coefficient, water solubility, antioxidant capacity, photochemical stability, and potential photoactivity.

EXPERIMENTAL SECTION

Extraction Procedure. Bixin was extracted from food grade annatto powder and from annatto seeds obtained from the University of Ghana Botanical Gardens and from the Brong Ahafo Region of Ghana. Bixin was extracted from annatto powder/seeds using a Soxhlet apparatus, based on the procedure of Silva et al.³² Hexane was first used to “wash” the seeds for about 170 h to remove unwanted oils. This was followed with chloroform to extract the bixin. The solvent was removed from the extract using a rotavap, leaving behind a dry mass. The dry mass was then redissolved in chloroform/acetone (2:1) in a flask, wrapped in Al-foil, and cooled to ~10 °C to precipitate bixin out of the solution. The precipitate was then filtered, yielding less than 0.5% of the mass of the annatto seeds of which only a small fraction is the bixin containing seed coat. NMR measurements showed that the product contained a 80:20 mixture of *cis* and *trans* isomers and will be referred to as bixin unless otherwise noted in the rest of this paper. Some isomerization presumably occurred during the heating/extraction process. HPLC-grade hexane and acetone were purchased from Alfa Aesar and HPLC grade chloroform from Fisher.

Radical Preparation. Silica–alumina (Si–Al) grade 135 ($Al_2O_3 = 13\%$ particle size distribution, 100 mesh) with a total pore volume and surface area of 0.640 mL/g and 447.67 m²/g, respectively, was purchased from Aldrich chemical company. Si–Al was activated at 700 °C for 7 h and quickly transferred to a nitrogen drybox and stored in the oxygen and water-free environment. To prepare the bixin solutions, ~0.74 mg of bixin was dissolved in chloroform and evaporated to a dry film in an amber vial which was evacuated and transferred into the drybox. The bixin film was dissolved in 1.4 mL of dry chloroform that had previously been purified on a column of basic alumina³³ and stored over an activated 3 Å molecular sieve. Three samples were prepared by adding 600 μ L of bixin solution: ~0.134, ~0.089, and ~0.030 mM to 4 mm quartz Norell EPR-250S tubes which were then connected to a vacuum line. The solution was degassed by five freeze–pump–thaw cycles and then transferred under a vacuum into the drybox. Activated Si–Al was added to each EPR tube. As the activated Si–Al settled to the bottom of the tube and adsorbed the bixin, the solution became colorless. Each tube was transferred without exposure to air to the vacuum line. This prevented deactivation of the Si–Al by water or oxygen. The solvent was removed by sublimation for 4 h and was evacuated overnight. The Si–Al became onyx black in color as the last of the solvent was removed. The EPR tubes were sealed under a vacuum using a natural gas/oxygen torch with the sample submerged in liquid nitrogen.

EPR and ENDOR. The EPR and ENDOR spectra of the sample were recorded before and after visible light irradiation. The sample was irradiated with a Y1711 Xe arc lamp through filters to remove UV and IR. The filtered light was focused onto the sample immersed in liquid nitrogen. Continuous wave (CW) EPR measurements were made at 77 K using a Bruker ELEXYS E540 CW X-band EPR spectrometer. The pulsed X-band ENDOR experiments were made with a Bruker ELEXYS E-680W/X EPR spectrometer in an EN 4118X-MD4-W1 resonator in a Flexline cryostat with an ENI A-500 RF power amplifier using the Mims ENDOR ($\pi/2-\tau-\pi/2-T-\pi/2-\tau$ -echo) pulse sequence with a 10 μ s RF π -pulse applied during the delay time T . ENDOR spectra were recorded at two different values of τ : 200 and 400 ns. The Mims ENDOR spectra are plotted as the ENDOR effect which is the change in echo intensity with RF on and off resonance divided by the echo intensity with the RF off resonance. The Davies ENDOR pulse sequence ($\pi-T-\pi/2-\tau-\pi-\tau$ -echo) had a 10 μ s RF π -pulse applied during the time period T with $\tau = 400$ ns and a microwave π pulse of 240 ns. Stochastic ENDOR data collection was used for both types of ENDOR. The experimental ENDOR spectra have a noticeable intensity imbalance for positive and negative frequency shifts due to imperfections in the matching of our ENDOR coil. This imbalance is considered during spectral fitting.

DFT Calculations. DFT calculations were carried out with the Gaussian 09 program package³⁴ on the SGI UV and DMC computers at the Alabama Supercomputer Center. Optimization of the molecular geometry was made at the DFT level with the B3LYP exchange-correlation functional^{35,36} and the 6-31G** basis set,³⁷ which we have previously shown is reasonable for predicting the geometry of β -carotene based radicals.³⁸ Single point calculations at these geometries were used to predict hyperfine couplings at the B3LYP level with the TZP basis set from Ahlrichs' group³⁹ which agree well with EPR experimental data for other carotenoids.^{24,38,40} No attempt was made to model the interaction with Si-Al or neighboring carotenoid molecules because they have little effect in other carotenoids and because the atomic structure and location of Si-Al activated sites are poorly characterized. Ampac 10.1 from Semichem that includes Graphical User Interface (AGUI) was used to visualize the DFT unpaired spin densities.

ENDOR Spectral Simulation Methods. Mims ENDOR spectra simulation was made using EasySpin⁴¹ in Matlab (MathWorks). The isotropic and anisotropic components of the ^1H hyperfine couplings²⁷ and the direction cosine matrix, \mathbf{R} , from the Gaussian output files were imported into Matlab. The hyperfine tensor, \mathbf{T} , of each ^1H was constructed as a diagonal tensor. In the case of the methyl ^1H , each hyperfine tensor was then rotated into the molecular axis frame by a unitary transformation with its direction cosine matrix, $\mathbf{R}^{-1} \cdot \mathbf{T} \cdot \mathbf{R}$. The tensors of the three methyl ^1H were averaged to a single tensor, as appropriate for rapidly rotating methyl groups, and its principal values were used for simulation with a weighting of three times that of single ^1H . Mims ENDOR can be simulated accurately; for an example, see ref 42.

CW ENDOR simulations were also made as an approximation of the Davies ENDOR spectra.²⁴ Davies ENDOR is subject to a number of distortions that are difficult to characterize and quantitate. Doan et al.^{43–45} have described the dependence of Davies ENDOR intensity on the product of microwave pulse width and hyperfine coupling with an optimum occurring when the product is ~ 0.7 and with the

intensity going to zero when that product is small. There are also artifacts and distortions caused by spectral diffusion and the microwave excitation profiles that are difficult to predict accurately. However, the Davies ENDOR spectra are more attractive to view because the distortions, even when large, are not as glaring as the Mims blind spots.

RESULTS

EPR and ENDOR. The CW EPR spectrum of the bixin sample at 77 K consists of a strong, single, symmetric line, nearly Gaussian in shape, with a line width of 1.62 mT and $g_{\text{iso}} = 2.002$. The EPR spectrum is similar to those of other carotenoids.^{27,46,47} Irradiation by visible light caused a 4–5-fold decrease in intensity with no change in shape or position, from further photochemical reaction of the rather reactive bixin radicals, Figure 2. The major contribution to the line shape of

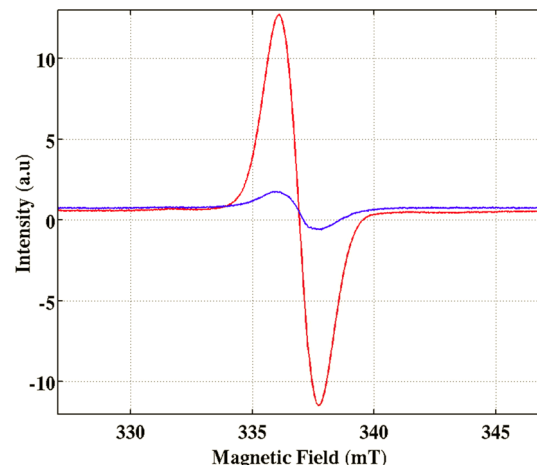


Figure 2. CW EPR spectrum at 77 K before irradiation (red) with a line width of 1.62 mT and $g_{\text{iso}} = 2.002$ and after 10 min of visible light irradiation (blue) with a 4–5-fold decrease in intensity.

carotenoid radicals at the X-band is unresolved hyperfine interactions with protons of the radical. The g -factor of typical carotenoid radicals is axially symmetric with an anisotropy⁴⁶ amounting to ~ 4.5 MHz at the X-band. The g -factor anisotropy is negligible compared to the inhomogeneous broadening from hyperfine interactions and does not produce any detectable orientation selection that is so prominent in many metalloproteins and metal ion complexes or in high-field EPR.⁴⁸

The Mims ^1H ENDOR spectra, plotted as the absolute ENDOR effect, are the same before and after irradiation, Figure 3. The free radical composition of the sample and the normalized ENDOR effect were not changed by visible light irradiation, although the absolute number of radicals changed. The ^1H ENDOR spectra extended well beyond ± 8 MHz, perhaps as far as ± 10 MHz, around the ^1H Larmor frequency, just below 15 MHz, with a shape indicating a large number of different hyperfine couplings contributing to the spectrum. The ^1H ENDOR spectra are similar to those from other carotenoids that form mixtures of radical cations and neutral radicals by loss of H^+ from the radical cations.^{24–26} The Mims ENDOR spectra at $\tau = 200$ and 400 ns appear rather different at first because of the different periodicity of the blind spots. However, their peaks, where the intensity is unaffected by the blind spot phenomenon, trace out the same envelope with very similar intensity because spectral diffusion (according to the

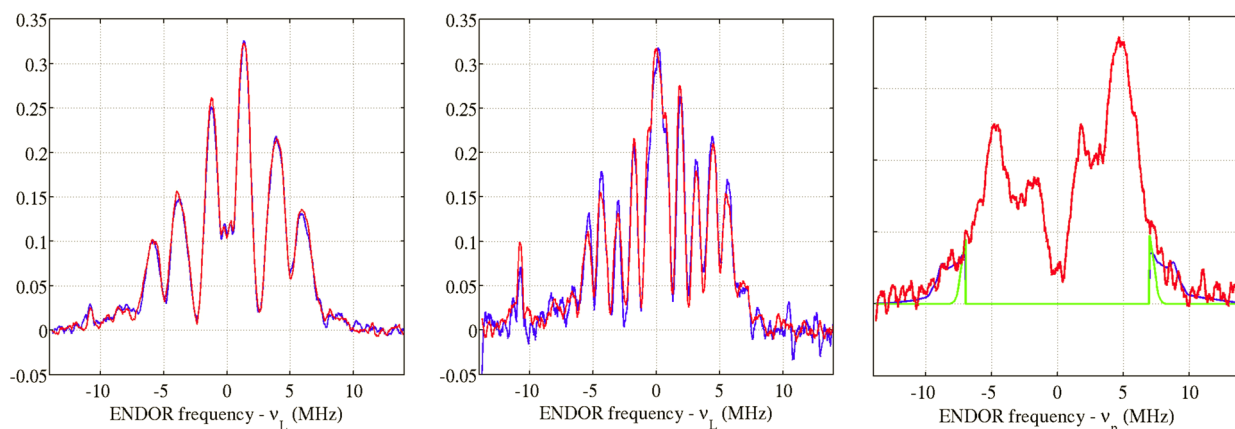


Figure 3. ENDOR spectra of bixin radicals on Si-Al. Left: Mims ^1H ENDOR spectra at $\tau = 200$ ns before (red) and after irradiation (blue) of the absolute ENDOR effect showing no change in free radical composition after 10 min of visible light irradiation. There is a small artifactual peak near -11 MHz. Center: Mims ^1H ENDOR spectra at $\tau = 400$ ns of the absolute ENDOR effect. Right: Davies ENDOR spectrum with $\tau = 400$ ns. There are two strong artifactual dips in the spectrum near ± 2.5 MHz caused by sinc function wiggles from the inverting microwave pulse. The sinc wiggles may cause an additional alteration of intensity near ± 5 MHz. The green spectrum represents the location of radical cations, and the blue spectrum is where the bixin neutral radicals occur. It is clear that neutral radicals are formed from the Davies ENDOR and is consistent with the presence of radical cations and neutral radicals deduced from the Mims ENDOR using DFT derived couplings.

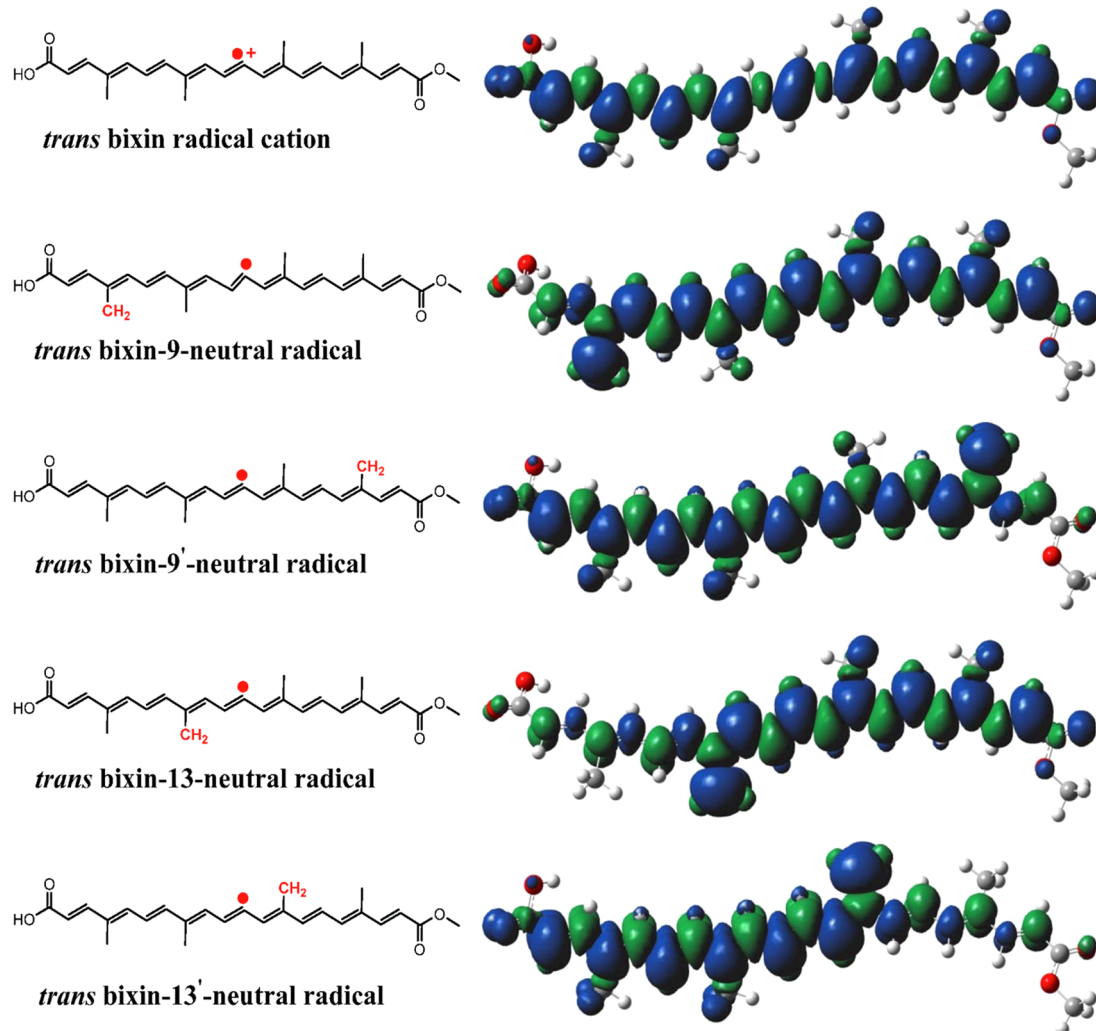


Figure 4. *trans* bixin radical cation and *trans* bixin neutral radicals. The chemical structure is shown on the left and the geometric structure with the unpaired spin density distribution on the right. The blue represents excess α and the green excess β unpaired spin density. The carbon atoms are gray, the oxygen atoms are red, and the hydrogen atoms are white.

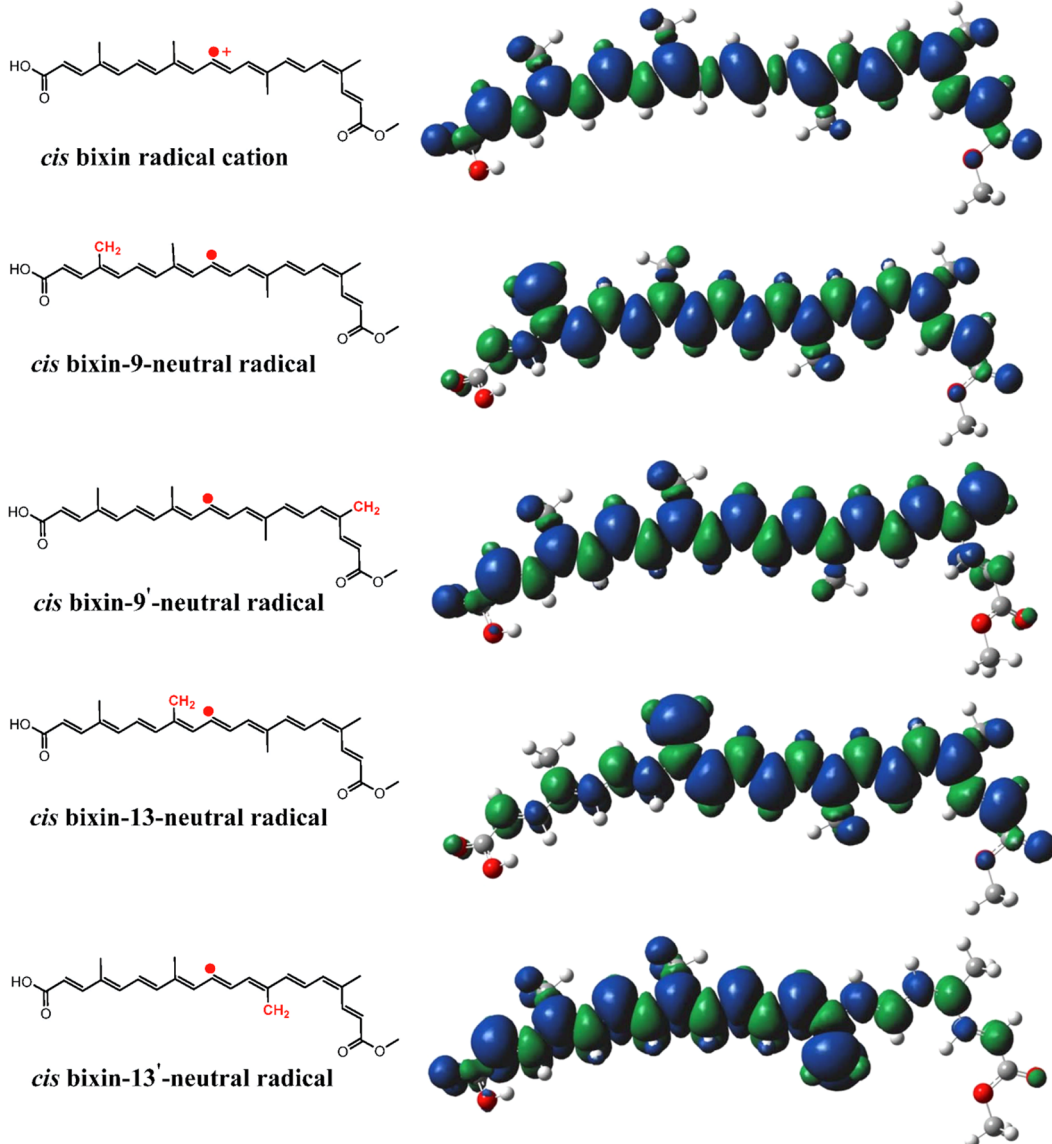


Figure 5. *cis* bixin radical cation and *cis* bixin neutral radicals. The chemical structure is shown on the left and the geometric structure with the unpaired spin density distribution on the right.

established models^{49,50} and other spin relaxation processes are completely corrected during the calculation of the absolute ENDOR effect, affecting the signal-to-noise ratio but not the shape or intensity of the spectrum.

The Davies ENDOR spectrum has more noise than the Mims ENDOR spectra even with greater measurement time. There is a hole in the center of the spectrum with a shape determined in part by sinc wiggles from the inverting microwave pulse that extend to ± 5 MHz and some spectral diffusion. The tails of the Davies ENDOR beyond ± 5 MHz appear consistent with the Mims ENDOR intensity at $\tau = 200$ and 400 ns, although the noise is rather large, indicating that the two sets of spectra are observing a similar set of radicals and hyperfine couplings. The Davies ENDOR spectra before and after irradiation did not show spectral changes distinguishable from the noise.

DFT Calculations. The initial radicals produced by electron transfer from carotenoid to Lewis acid sites on the activated Si-Al are radical cations. In general, there is facile H⁺ loss from the radical cations if there are H⁺ acceptors available. NMR

measurements of the bixin used to prepare samples showed the presence of ~20% *trans* bixin, so DFT calculations were carried out on possible radical products with *trans* and *cis* conformations. The *trans* and *cis* bixin radical cation geometries were optimized by DFT, and the hyperfine tensors were calculated at the optimum geometry. The Si-Al surface sites that stabilize carotenoid radicals are uncharacterized because no carotenoid radical has shown a measurable effect on its electron spin distribution or hyperfine couplings.^{24–29} The matrix proton ENDOR line from ¹H on surface –OH sites of Si-Al in all studies of carotenoid radicals^{24–29} is featureless and shows no strong specific interaction between the electron spin and any surface atom. The Si-Al surface was not included in the DFT calculations because it has not been characterized and because our previous studies failed to detect any influence of the surface on the EPR properties of other carotenoid radicals.²⁹ The optimized structure and unpaired spin density distributions are given in Figure 4 for the *trans* and Figure 5 for the *cis* configuration. Neutral radicals are formed by H⁺ loss from the 9(9') or 13(13') methyl groups of the *trans* and *cis* radical

Table 1. Relative Energies ΔE (kcal/mol) of *trans* and *cis* Bixin Neutral Radicals

radical	<i>trans</i> 9	<i>cis</i> 9	<i>trans</i> 9'	<i>cis</i> 9'	<i>trans</i> 13	<i>cis</i> 13	<i>trans</i> 13'	<i>cis</i> 13'
ΔE	2.25	3.54	2.04	0.00	3.30	4.54	3.25	4.16

cations. Their geometries were optimized to yield the structure and unpaired spin density distribution for the *trans* 9(9') and 13(13') neutral radicals given in Figure 4 and the *cis* 9(9') and 13(13') neutral radicals in Figure 5. The *trans* radical cation is more stable than the *cis* by 1.26 kcal/mol, Table 2. The *cis* 9'

Table 2. Relative Energies ΔE (kcal/mol) of *trans* and *cis* Cations

radical	<i>trans</i>	<i>cis</i>
ΔE	0.00	1.26

neutral radical is the most stable neutral radical, while the *cis* 13 neutral radical is the least stable by 4.54 kcal/mol, Table 1. Table S1 in the Supporting Information gives the DFT E(UB3LYP) energies, and Table S2 (Supporting Information) gives the relative energies in ascending order.

The anisotropic and isotropic coupling constants from DFT calculations are given in Tables S3–S22 (Supporting Information), and the atom numbers and labels from the DFT calculations and their corresponding positions in the bixin nomenclature are given in Tables S23–S25 (Supporting Information). The methyl groups of carotenoid radicals are rapidly rotating even at 4 K,⁴⁶ so their hyperfine tensors were averaged. The principal values of the averaged tensors are listed in Table S26 (Supporting Information). The cation and neutral radicals have little spin contamination with S^2 of 0.75 and 0.76, respectively. Tables S27 and S28 (Supporting Information) provide the S^2 of the neutral radicals and radical cations before and after annihilation, respectively. The ENDOR spectra were simulated using the DFT hyperfine tensors for all ¹H except intact methyl groups, where the averaged tensors were used for the bixin radical cations and neutral radicals, Figures S1–S12 (Supporting Information). The simulated ENDOR spectra of the *cis* and *trans* bixin radical cations are relatively narrow, extending only to $\sim \pm 7$ MHz, while the spectra of the neutral radicals all extend beyond ± 12 MHz. This pattern appears in other carotenoid radicals.^{24,25,40,51} The unpaired electron in

radical cations is delocalized over the entire conjugation length of the carotenoid, resulting in less spin density and weaker hyperfine couplings than in the neutral radicals where the conjugation is interrupted at the site of H⁺ loss, Figures 4 and 5. The unpaired spin density in neutral radicals is spread over fewer atoms, resulting in some hyperfine couplings being significantly larger than any found in the radical cation. The 13(13') neutral radicals have even shorter conjugation lengths than the 9(9') neutral radicals and have larger couplings and greater ENDOR intensity beyond ± 8 MHz, Table 3 and Figures S3–S12 (Supporting Information). The terminal polar groups that make bixin water-soluble do not significantly alter the spin distribution from that seen in the water-insoluble carotenoids.

Linear combinations of the simulated ENDOR spectra were used to obtain a global fit to the experimental ENDOR spectra at $\tau = 200$ and 400 ns. For fitting, the center of the ENDOR spectrum within ± 3 MHz was discounted because the experimental spectrum contains intensity from weakly coupled ¹H external to the bixin radical that are not included in the DFT calculations or simulations. The fitting is an under-determined problem because some of the simulated spectra are virtually indistinguishable from each other and their individual contributions to the spectrum could not be determined. In particular, the *trans* 9 and *trans* 9' neutral radicals are >94% identical and cannot be distinguished from each other. This problem is quite understandable because the two radicals only differ by the location of the methyl ester which has virtually no unpaired spin density. The radical cations have similar spectra, but there is a noticeable difference near ± 7 MHz that provides an ability to distinguish the contributions from both radicals but leads to highly correlated uncertainties in their amounts. However, the differences in overall width of the ENDOR spectrum, whether measured using Mims or Davies ENDOR, allow the radical cation contribution to be reliably distinguished from those of the neutral radicals.

The fits of ENDOR spectra from four different samples, Table 3, find strongly correlated uncertainties between amounts

Table 3. Spectral Fits and Error Analysis of All Ten Radicals: *trans* and *cis* Radical Cations and 8 Neutral Radicals (9, 9', 13, and 13' *cis* and *trans*)

radicals	<i>trans</i> 9, 9'	<i>cis</i> 13'	<i>trans</i> 13, 13'	<i>trans</i> cation	<i>cis</i> cation	<i>cis</i> 9	<i>cis</i> 9'	<i>cis</i> 13	RMS error	
fit 1	%	15	0	25	18	33	0	2	7	0.032322
fit 2	%	14	0	30	27	16	0	8	6	0.033910
fit 3	%	4	0	26	31	21	0	10	9	0.032050
fit 4	%	15	1	24	29	21	0	3	8	0.033912
mean		12	0	26	26	23	0	6	8	
STDV		4.6	0.4	2.3	5.0	6.3	0.0	3.3	1.1	
total neutrals and cations										
radicals				<i>trans</i> cation				<i>cis</i> cation	neutrals	
fit 1				18				33	49	
fit 2				27				16	58	
fit 3				31				21	49	
fit 4				29				21	51	
mean				26				23	52	
STDV				5.0				6.3	3.7	

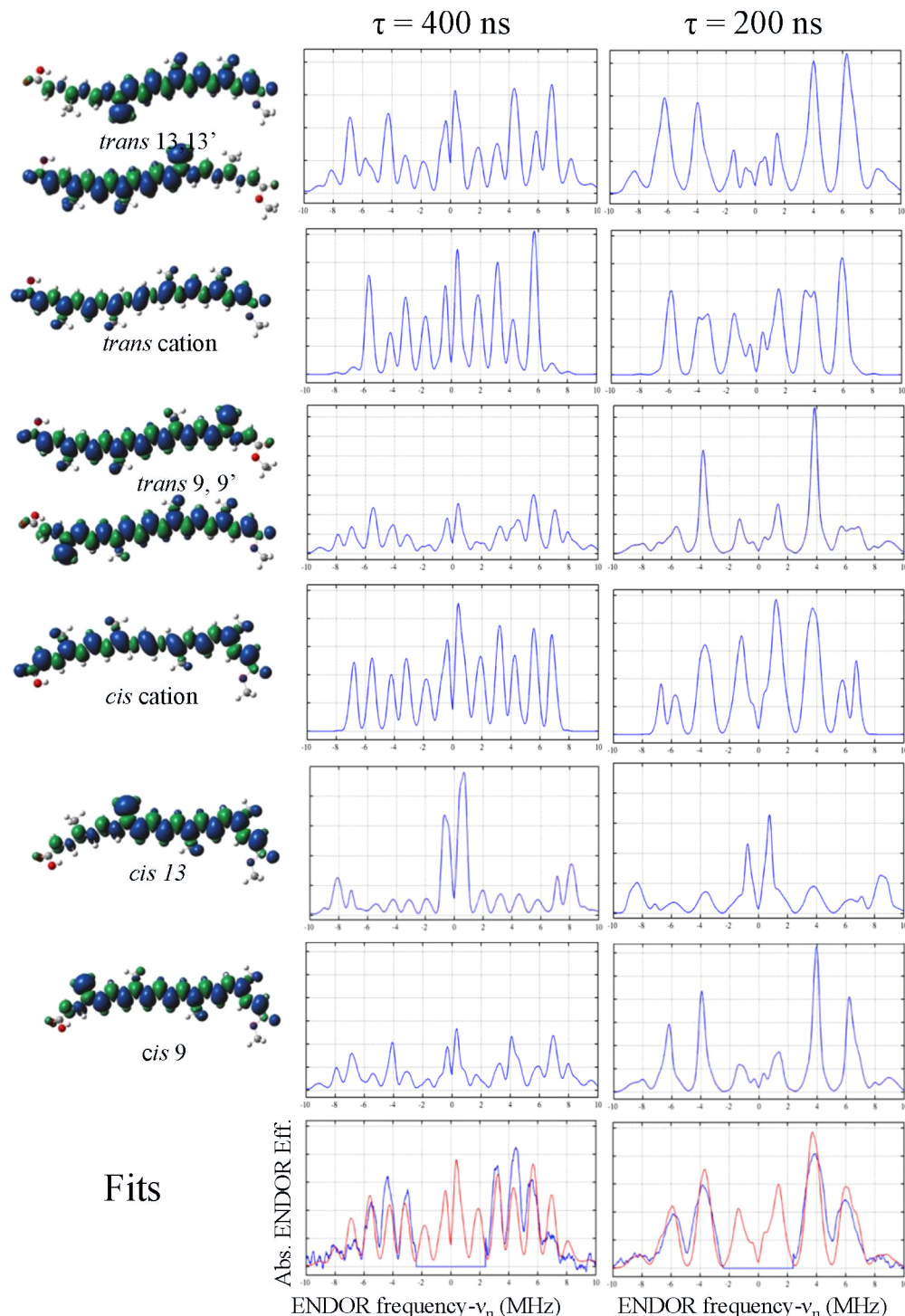


Figure 6. Spin densities (left) and simulated Mims ENDOR spectra (right) of radicals that contribute to the EPR spectrum and the fits at $\tau = 200$ and 400 ns. The black trace is the experimental spectrum with the discounted central portion omitted. ENDOR parameters: $T = 20$ K, $B = 347.5$ mT, $\nu = 9.76$ GHz. The blue is the resultant simulation.

of some species because of the strong similarity of their spectra. There is strong, consistent agreement in the spectra from all four samples that half the radicals are radical cations and the other half are neutral radicals from ^1H loss from one of the methyl groups. Among the neutral radicals, *trans* and *cis* conformations are in a 3:1 ratio, which is different from the starting material (1:4 ratio) applied to the Si-Al.

The fit is confirmed by visual examination of the experimental spectra, Figure 6, beyond ± 8 MHz from the ^1H

Larmor frequency. Weak but definite spectral intensity is present that cannot come from the radical cations which have no intensity in that region. This requires the presence of neutral radicals. The far wings of the experimental spectrum beyond ± 8 MHz are less intense than those for any of the neutral radicals which indicate substantial amounts of radical cations. Thus, the results of the fit are consistent with the overall shape of the experimental spectrum.

■ DISCUSSION

The *trans* radical cation of bixin is more stable than the *cis* form by 1.25 kcal/mol or only 2 kT at 300 K. The most stable bixin neutral radical is the *cis* 9' conformation, with the *trans* 9' and 9 next most stable by just 4 kT or ~2.1 kcal/mol. The spectral fit found 26% *cis* bixin and 23% *trans* bixin radical cation which is consistent with the small difference in energy between the *cis* and *trans* conformations predicted by DFT calculations, but the ratio of *cis:trans* radical cations from the spectral fit has a large uncertainty because of the strong similarity between the simulated spectra.

Other carotenoids form neutral radicals on Si-Al whose relative gas phase energies are even greater than 4.5 kcal/mol. They include neutral radicals of zeaxanthin (Zea), violaxanthin (Viol),²⁴ and astaxanthin (Ast).²⁵ Zea and Viol²⁴ adsorbed on Si-Al produce radical cations and also a neutral carotenoid radical by H⁺ loss at the 4(4') methylene position, as well as from methyl groups at 5(5'), 9(9'), and 13(13') for Zea and at 9(9') and 13(13') for Viol.

For Ast²⁵ supported on activated Si-Al, an equal distribution of Ast^{•+}, 3b[Ast-H][•], 5[Ast-H][•], 9[Ast-H][•], and 13[Ast-H][•] was able to fit the ENDOR spectrum. This occurred even though the relative gas phase energies of the neutral radicals varied from 0 to 4.68, to 13.74, to 14.03, to 15.9 kcal/mol, respectively. This relative energy difference is much larger than what is seen for bixin (Tables 1 and 2).

Interestingly, the ratio of *trans* to *cis* isomers in the neutral radicals was not similar to the applied bixin (20% *trans* to 80% *cis*) where the *cis* isomer is the ground state structure. Isomerization at double bonds is facile in carotenoid radical cations, leading to an accumulation of the *trans* carotenoid.^{29,52} The apparent isomerization among the neutral radicals (74% *trans* and 26% *cis*) suggests that electron transfer to form the radical cation occurs before bixin binds to the Si-Al surface and that the neutral radical product is much less prone to isomerize than the radical cation or is sterically prevented from doing so by its environment on the Si-Al.

The effort to make carotenoids water-soluble⁵³ so that they can be administered in water and readily absorbed from the gut faces a dilemma. Altering such fundamental properties as polarity and solubility may also radically change the very properties that make carotenoids desired: their ability to scavenge free radicals, to serve as antioxidants, and to serve as electron donors. In bixin, we find that water solubility has not produced major changes to its free radical properties. Despite the presence of very polar carboxyl and ester groups, we find free radical chemistry and properties similar to the other carotenoids we have studied. Bixin undergoes the same electron transfer reactions to form a radical cation under the same conditions as other water-insoluble carotenoids. The radical cation readily transfers H⁺ to an acceptor, forming a neutral radical under similar conditions. The spin distribution and hyperfine couplings of the radical cation are typical of those of other carotenoids. The neutral radicals have shorter conjugation and larger hyperfine couplings than the radical cations, as do other carotenoids. In short, all the free radical properties, electron transfer reactions, and radical chemistry that we examined in bixin were preserved intact despite the major change in its solubility and polarity. Bixin is the first natural, water-soluble carotenoid to be characterized in this way and suggests that chemically modified or synthetic carotenoids may also achieve a similar combination of properties.

■ ASSOCIATED CONTENT

Supporting Information

trans and *cis* bixin radical unpaired spin densities and their respective conformations (Figures S1 and S2) derived from DFT calculations. The total energies of all 10 radicals (in Hartree and kcal/mol) (Tables S1 and S2) and their respective calculated hyperfine coupling tensors using B3LYP/6-31(d,p) (Tables S3–S26). The simulated spectra for each individual radical conformation (*cis* and *trans*) at τ = 200 and 400 ns are listed in Figures S3–S12. This material is available free of charge via the Internet at <http://pubs.acs.org>.

■ AUTHOR INFORMATION

Corresponding Author

*E-mail: lkispert@ua.edu

Present Address

[†]M.D.K.: Department of Chemistry, Northwestern University, Evanston, IL.

Notes

The authors declare no competing financial interest.

■ ACKNOWLEDGMENTS

This work was supported in part by the Chemical Sciences, Geosciences, and Biosciences Division, Office of Basic Sciences, U.S. Department of Energy, Grant DE-FG02-86ER-13465 which provided RA support for S.S.T.-A. and supplies and support for the P.I. L.D.K. The DFT calculations were carried out using the resources provided by the Alabama Supercomputer Center. The EPR measurements were made possible by the National Science Foundation for EPR Instrument Grants CHE-0342921 and CHE-0079498 to UA. The expert assistance of Alex Cruce in fitting of the calculated to the experimental ENDOR was greatly appreciated and led to an improved manuscript.

■ REFERENCES

- Preston, H.; Rickard, M. Extraction and chemistry of annatto. *Food Chem.* **1980**, *5*, 47–56.
- Dias, V. M.; Pilla, V.; Alves, L. P.; Oliveira, H. P.; Munin, E. Optical Characterization in Annatto and Commercial Colorific. *J. Fluoresc.* **2011**, *21*, 415–421.
- Balaswamy, K.; Prabhakara Rao, P.; Satyanarayana, A.; Rao, D. Stability of bixin in annatto oleoresin and dye powder during storage. *LWT—Food Sci. Technol.* **2006**, *39*, 952–956.
- Barbosa, M.; Borsarelli, C.; Mercadante, A. Light stability of spray-dried bixin encapsulated with different edible polysaccharide preparations. *Food Res. Int.* **2005**, *38*, 989–994.
- Mercadante, A.; Steck, A.; Pfander, H. Isolation and identification of new apocarotenoids from annatto (*Bixa orellana*) seeds. *J. Agric. Food Chem.* **1997**, *45*, 1050–1054.
- Chisté, R. C.; Benassi, M. T.; Mercadante, A. Z. Effect of solvent type on the extractability of bioactive compounds, antioxidant capacity and colour properties of natural annatto extracts. *Int. J. Food Sci. Technol.* **2011**, *46*, 1863–1870.
- Satyanarayana, A.; Prabhakara Rao, P.; Rao, D. Chemistry, processing and toxicology of annatto (*Bixa orellana* L.). *J. Food Sci. Technol.* **2003**, *40*, 131–141.
- Mercadante, A.; Steck, A.; Rodriguez-Amaya, D.; Pfander, H.; Britton, G. Isolation of methyl 9' Z-apo-6'-lycopenoate from *Bixa orellana*. *Phytochemistry* **1996**, *41*, 1201–1203.
- Scotter, M. The chemistry and analysis of annatto food colouring: a review. *Food Addit. Contam.* **2009**, *26*, 1123–1145.

- (10) Gao, F. G.; Bard, A. J.; Kispert, L. D. Photocurrent generated on a carotenoid-sensitized TiO₂ nanocrystalline mesoporous electrode. *J. Photochem. Photobiol., A* **2000**, *130*, 49–56.
- (11) Rios, A. d. O.; Mercadante, A. Z.; Borsarelli, C. D. Triplet state energy of the carotenoid bixin determined by photoacoustic calorimetry. *Dyes Pigm.* **2007**, *74*, 561–565.
- (12) Chisté, R. C.; Mercadante, A. Z.; Gomes, A.; Fernandes, E.; da Costa Lima, J. L. F.; Bragagnolo, N. In vitro scavenging capacity of annatto seed extracts against reactive oxygen and nitrogen species. *Food Chem.* **2011**, *127*, 419–426.
- (13) Montenegro, M. A.; Rios, A. d. O.; Mercadante, A. Z.; Nazareno, M. A.; Borsarelli, C. D. Model studies on the photosensitized isomerization of bixin. *J. Agric. Food Chem.* **2004**, *52*, 367–373.
- (14) Zsila, F.; Molnár, P.; Deli, J.; Lockwood, S. F. Circular dichroism and absorption spectroscopic data reveal binding of the natural *cis*-carotenoid bixin to human α_1 -acid glycoprotein. *Bioorg. Chem.* **2005**, *33*, 298–309.
- (15) Lyng, S. M. O.; Passos, M.; Fontana, J. D. Bixin and α -cyclodextrin inclusion complex and stability tests. *Process Biochem.* **2005**, *40*, 865–872.
- (16) Satyanarayana, A.; Prabhakara Rao, P.; Balaswamy, K.; Velu, V.; Rao, D. G. Application of annatto dye formulations in different fruit and vegetable products. *J. Foodservice* **2006**, *17*, 1–5.
- (17) Silva, G.; Gamarra, F.; Oliveira, A.; Cabral, F. Extraction of bixin from annatto seeds using supercritical carbon dioxide. *Braz. J. Chem. Eng.* **2008**, *25*, 419–426.
- (18) Liu, D.; Gao, Y.; Kispert, L. D. Electrochemical properties of natural carotenoids. *J. Electroanal. Chem.* **2000**, *488*, 140–150.
- (19) Magyar, A.; Bowman, M. K.; Molnár, P.; Kispert, L. Neutral Carotenoid Radicals in Photoprotection of Wild-Type *Arabidopsis thaliana*. *J. Phys. Chem. B* **2013**, *117*, 2239–2246.
- (20) Hernandez-Marin, E.; Galano, A.; Martinez, A. Cis carotenoids: colorful molecules and free radical quenchers. *J. Phys. Chem. B* **2013**, *117*, 4050–4061.
- (21) Rusina, I.; Karpukhin, O.; Kasaikina, O. Chemiluminescent methods for studying inhibited oxidation. *Russ. J. Phys. Chem. B* **2013**, *7*, 463–477.
- (22) Crépeau, G.; Montouillout, V.; Vimont, A.; Mariey, L.; Cseri, T.; Maugé, F. Nature, structure and strength of the acidic sites of amorphous silica alumina: an IR and NMR study. *J. Phys. Chem. B* **2006**, *110*, 15172–15185.
- (23) Bhaduri, S.; Mukesh, D. In *Chemical Industry and Homogeneous Catalysis: Mechanisms and Industrial Applications; Homogeneous Catalysis*; John Wiley & Sons, Inc: New York, 2000; pp 1–12.
- (24) Focsan, A. L.; Bowman, M. K.; Konovalova, T. A.; Molnár, P.; Deli, J.; Dixon, D. A.; Kispert, L. D. Pulsed EPR and DFT characterization of radicals produced by photo-oxidation of zeaxanthin and violaxanthin on silica-alumina. *J. Phys. Chem. B* **2008**, *112*, 1806–1819.
- (25) Polyakov, N. E.; Focsan, A. L.; Bowman, M. K.; Kispert, L. D. Free radical formation in novel carotenoid metal ion complexes of astaxanthin. *J. Phys. Chem. B* **2010**, *114*, 16968–16977.
- (26) Focsan, A. L.; Bowman, M. K.; Shamshina, J.; Krzyaniak, M. D.; Magyar, A.; Polyakov, N. E.; Kispert, L. D. EPR Study of the Astaxanthin n-Octanoic Acid Monoester and Diester Radicals on Silica-Alumina. *J. Phys. Chem. B* **2012**, *116*, 13200–13210.
- (27) Konovalova, T. A.; Dikanov, S. A.; Bowman, M. K.; Kispert, L. D. Detection of anisotropic hyperfine components of chemically prepared carotenoid radical cations: 1D and 2D ESEEM and pulsed ENDOR study. *J. Phys. Chem. B* **2001**, *105*, 8361–8368.
- (28) Jeevarajan, A. S.; Kispert, L. D.; Piekara-Sady, L. An ENDOR study of carotenoid cation radicals on silica—alumina solid supports. *Chem. Phys. Lett.* **1993**, *209*, 269–274.
- (29) Kispert, L. D.; Polyakov, N. E. Carotenoid Radicals: Cryptochemistry of Natural Colorants. *Chem. Lett.* **2010**, *39*, 148–155.
- (30) Samoilova, R. I.; Shubin, A. A.; Bowman, M. K.; Hüttermann, J.; Dikanov, S. A. Observation of two paramagnetic species in electron transfer reactions within cesium modified X and Y zeolites. *Chem. Phys. Lett.* **2000**, *316*, 404–410.
- (31) Samoilova, R. I.; Dikanov, S. A.; Fionov, A. V.; Tyryshkin, A. M.; Lunina, E. V.; Bowman, M. K. Pulsed EPR study of orthophosphoric and boric acid modified γ -alumina. *J. Phys. Chem.* **1996**, *100*, 17621–17629.
- (32) Silva, M. C.; Botelho, J.; Conceição, M. M.; Lira, B.; Coutinho, M. A.; Dias, A.; Souza, A.; Filho, P. Thermogravimetric investigations on the thermal degradation of bixin, derived from the seeds of annatto (*Bixa orellana* L.). *J. Therm. Anal. Calorim.* **2005**, *79*, 277–281.
- (33) Armarego, W. L.; Chai, C. In *Purification of Organic Chemicals-Aliphatic Compounds; Purification of laboratory chemicals*; Butterworth-Heinemann: Burlington, 2012; p 116.
- (34) Frisch, M. J.; Trucks, G. W.; Schlegel, H. B.; Scuseria, G. E.; Robb, M. A.; Cheeseman, J. R.; Scalmani, G.; Barone, V.; Mennucci, B.; Petersson, G. A.; Nakatsuji, H.; Caricato, M.; Li, X.; Hratchian, H. P.; Izmaylov, A. F.; Bloino, J.; Zheng, G.; Sonnenberg, J. L.; Hada, M.; Ehara, M.; Toyota, K.; Fukuda, R.; Hasegawa, J.; Ishida, M.; Nakajima, T.; Honda, Y.; Kitao, O.; Nakai, H.; Vreven, T.; Montgomery, J. A., Jr.; Peralta, J. E.; Ogliaro, F.; Bearpark, M.; Heyd, J. J.; Brothers, E.; Kudin, K. N.; Staroverov, V. N.; Kobayashi, R.; Normand, J.; Raghavachari, K.; Rendell, A.; Burant, J. C.; Iyengar, S. S.; Tomasi, J.; Cossi, M.; Rega, N.; Millam, N. J.; Klene, M.; Knox, J. E.; Cross, J. B.; Bakken, V.; Adamo, C.; Jaramillo, J.; Gomperts, R.; Stratmann, R. E.; Yazyev, O.; Austin, A. J.; Cammi, R.; Pomelli, C.; Ochterski, J. W.; Martin, R. L.; Morokuma, K.; Zakrzewski, V. G.; Voth, G. A.; Salvador, P.; Dannenberg, J. J.; Dapprich, S.; Daniels, A. D.; Farkas, Ö.; Foresman, J. B.; Ortiz, J. V.; Cioslowski, J.; Fox, D. J. *Gaussian 09*, revision D.02; Gaussian, Inc.: Wallingford, CT, 2009.
- (35) Becke, A. D. Density-functional thermochemistry. III. The role of exact exchange. *J. Chem. Phys.* **1993**, *98*, 5648–5652.
- (36) Lee, C.; Yang, W.; Parr, R. G. Development of the Colle-Salvetti correlation-energy formula into a functional of the electron density. *Phys. Rev. B* **1988**, *37*, 785.
- (37) Hehre, W. J.; Radom, L.; Schleyer, P. v. R.; Pople, J. A. *Ab initio molecular orbital theory*; Wiley: New York, 1986; Vol. 67.
- (38) Gao, Y.; Focsan, A. L.; Kispert, L. D.; Dixon, D. A. Density functional theory study of the β -carotene radical cation and deprotonated radicals. *J. Phys. Chem. B* **2006**, *110*, 24750–24756.
- (39) Schäfer, A.; Horn, H.; Ahlrichs, R. Fully optimized contracted Gaussian basis sets for atoms Li to Kr. *J. Chem. Phys.* **1992**, *97*, 2571–2577.
- (40) Focsan, A. L.; Bowman, M. K.; Molnár, P.; Deli, J.; Kispert, L. D. Carotenoid Radical Formation: Dependence on Conjugation Length. *J. Phys. Chem. B* **2011**, *115*, 9495–9506.
- (41) Stoll, S.; Schweiger, A. EasySpin, a comprehensive software package for spectral simulation and analysis in EPR. *J. Magn. Reson.* **2006**, *178*, 42–55.
- (42) Trukhan, S.; Yudanov, V.; Tormyshev, V.; Rogozhnikova, O. Y.; Trukhin, D.; Bowman, M.; Krzyaniak, M.; Chen, H.; Martyanov, O. Hyperfine interactions of narrow-line trityl radical with solvent molecules. *J. Magn. Reson.* **2013**, *233*, 29–36.
- (43) Telser, J. Electron Nuclear Double Resonance (ENDOR) Spectroscopy. In *Application of Physical Methods to Inorganic and Bioinorganic Chemistry*; Scott, R. A.; Lukehart, C. M., Eds. John Wiley & Sons: Chichester, 2007.
- (44) Doan, P. E.; Fan, C.; Davoust, C. E.; Hoffman, B. M. A simple method for hyperfine-selective heteronuclear pulsed ENDOR via proton suppression. *J. Magn. Reson.* **1991**, *95*, 196–200.
- (45) Fan, C.; Doan, P. E.; Davoust, C. E.; Hoffman, B. M. Quantitative studies of davies pulsed ENDOR. *J. Magn. Reson.* **1992**, *98*, 62–72.
- (46) Konovalova, T. A.; Krzystek, J.; Bratt, P. J.; Van Tol, J.; Brunel, L. C.; Kispert, L. D. 95–670 GHz EPR studies of canthaxanthin radical cation stabilized on a silica-alumina surface. *J. Phys. Chem. B* **1999**, *103*, 5782–5786.
- (47) Kispert, L. D.; Konovalova, T.; Gao, Y. Carotenoid radical cations and dications: EPR, optical, and electrochemical studies. *Arch. Biochem. Biophys.* **2004**, *430*, 49–60.
- (48) Dikanov, S. A.; Xun, L.; Karpiel, A. B.; Tyryshkin, A. M.; Bowman, M. K. Orientationally-selected two-dimensional ESEEM

spectroscopy of the Rieske-type iron-sulfur cluster in 2, 4, 5-trichlorophenoxyacetate monooxygenase from *Burkholderia cepacia* AC1100. *J. Am. Chem. Soc.* **1996**, *118*, 8408–8416.

(49) Mims, W. B. Electron Spin Echoes. In *Electron Paramagnetic Resonance*; Geschwind, S., Ed.; Plenum: New York, 1972; pp 263–352.

(50) Salikhov, K.; Semenov, A.; Tsvetkov, Y. D. *Electron Spin Echoes and Their Applications*; Nauka: Novosibirsk, Russia, 1976.

(51) Focsan, A. L.; Molnár, P.; Deli, J.; Kispert, L. Structure and Properties of 9'-cis Neoxanthin Carotenoid Radicals by Electron Paramagnetic Resonance Measurements and Density Functional Theory Calculations: Present in LHC II? *J. Phys. Chem. B* **2009**, *113*, 6087–6096.

(52) Gao, Y.; Kispert, L. D. Reaction of carotenoids and ferric chloride: Equilibria, isomerization, and products. *J. Phys. Chem. B* **2003**, *107*, 5333–5338.

(53) Polyakov, N. E.; Leshina, T. V.; Meteleva, E. S.; Dushkin, A. V.; Konovalova, T. A.; Kispert, L. D. Water Soluble Complexes of Carotenoids with Arabinogalactan. *J. Phys. Chem. B* **2009**, *113*, 275–282.